Electronic Supplementary Information

Molecular evidence of a toxic effect on a biofilm and its matrix

Yuanzhao Ding[a,b], Yufan Zhou[c], Juan Yao[a], Yijia Xiong[d], Zihua Zhu* [c], Xiao-Ying Yu* [a]

a. Earth and Biological Sciences Directorate, Pacific Northwest National Laboratory. Richland, Washington 99354, United States

b. Singapore Centre for Environmental Life Sciences Engineering (SCELSE), Nanyang Technological University, 637551, Singapore

c. Environmental and Molecular Science Laboratory, Pacific Northwest National Laboratory, Richland, WA 99352, USA

d. Western University of Health Sciences, Lebanon, OR 97355, USA

* Correspondence and requests for materials should be addressed to X.-Y.Y. (email: xiaoying.yu@pnnl.gov) or Z.Z. (email: zihua.zhu@pnnl.gov).

Keywords: biofilm • Shewanella oneidensis • CP2-1-S1 • SALVI • liquid ToF-SIMS • Toxicity • Molecular Imaging

CONTENTS

Electronic Supplementary Experimental Details 4
ToF-SIMS 4
Dry biofilm and dry MM1 sample preparation 4
Supplemental Figures 5
Figure S1. Fluorescence images of the biofilm in the microfluidic channels: (a) WT biofilm; (b) WT biofilm treated with Cr; (c) CP biofilm; and (d) CP biofilm treated with Cr. The white bar represents 20 μm. 5
Figure S2. Schematic of the in situ liquid ToF-SIMS analysis of S. oneidensis MR-1 biofilms. 6
Figure S3. (a) Depth profiling of the WT biofilm in the negative mode and (b) reconstructed liquid ToF-SIMS negative spectra. Red bars depict the location of water cluster peaks. 7
Figure S4. (a) Depth profiling of the untreated biofilm; (b) representative 2D images; (c) 3D images reconstructed from Region II in the negative depth profile. 8
Figure S5. Liquid ToF-SIMS spectra of all samples in the positive mode. Red bars depict the location of water cluster peaks 9
Figure S6. Liquid ToF-SIMS spectra of all samples in the negative mode. Red bars depict the location of water cluster peaks 10
Figure S7. The scores plot of PC1 vs. PC2 (a); PC1 vs. PC3 (b); PC1 vs. PC4 (c); PC1 vs. PC4 (d) in the positively selected peaks spectral PCA. The loadings plots of each PC are depicted in (e). Red bars indicate the location of water cluster peaks, purple quorum sensing signal peaks, and green fatty acid peaks. 11
Figure S8. The scores plots of PC1 vs. PC2 (a), PC1 vs. PC3 (b), PC1-PC4 (c), and PC3-PC5 (d) in the negative selected peaks spectral PCA. The loadings plots of each PC are depicted in (e). Red bars indicate the location of water cluster peaks, blue chromium reduction related peaks, purple quorum sensing signal peaks, and green fatty acid peaks. 12
Figure S9. Image PCA in the positive ion mode. (a) Reconstructed false-color 2D PCA images in RGB corresponding to each PC scores at these locations along the microfluidic channel in the positive mode. The RGB composite images of the three key PCs are depicted. (b) Image PCA loadings plots illustrating the contribution of the selective chemical species in positive ion mode. 13
Supplemental Tables 14
Table S1. Summary of sample descriptions 14
Table S2a. Dry biofilm sample mass to charge ratios in the positive ion mode. 15
Table S2b. Dry biofilm sample observed mass to charge ratios in the negative ion mode 16
Table S3a. Dry MM1 medium sample observed mass to charge ratios in the positive ion mode. 17
Table S3b. Dry MM1 medium sample observed mass to charge ratios in the negative ion mode. 17
Table S4a. List of peaks selected in the positive spectral PCA excluding no water cluster peaks. 18
Table S4b. List of water cluster peaks selected in the positive spectral PCA 20
Table S5a. List of peaks selected in the negative spectral PCA (non-water cluster). 21
Table S5b. List of peaks selected in the negative spectral PCA (water cluster). 23
Table S6a. List of peaks selected in the positive 2D image PCA excluding water cluster peaks. 24

Table S6b. List of water cluster peaks included in the positive 2D image PCA..... 26
Table S7a. List of peaks selected in the negative 2D image PCA excluding water cluster peaks..... 27
Table S7b. List of water cluster peaks included in the negative 2D image PCA (water cluster)..... 29
References..... 30

Electronic Supplementary Information

Supplemental information was provided to substantiate the discussion and provide additional experimental details including figures, tables, and associated references.

Electronic Supplementary Experimental Details

ToF-SIMS

ToF-SIMS V spectrometer (ION-TOF GmbH, Münster, Germany) was used in this study. Compared to earlier works,[3] optimized SIMS operation conditions were used.[4] The detailed comparison was described in another publication.[5] A 25 keV Bi_3^+ cluster ion beam was the primary ion beam in this study. During measurements, the Bi_3^+ beam was initially focused at around 200 nm diameter to obtain an observation area of 2 μm in diameter.[6] In each depth profile experiment (**Figure 2A**, region I), a wider pulse with a current of 1209 pA and cycle time of 30 μs was used initially before punching through the 100 nm SiN membrane. The punch-through time was approximately 360 s. After that the SiN membrane punch-through, a wider pulse was used for another 150 s to obtain spectra with a relatively better spatial resolution for image analysis (**Figure 2A**, region II). In the end, a narrower pulse width was used for another 200 s to obtain data with better mass resolution (**Figure 2A**, region III).

Dry biofilm and dry MM1 sample preparation

The biofilm was harvested in a tubular biofilm reactor. Each tubular biofilm reactor was made by the peroxide-cured silicone tubing (Masterflex, length 300 mm, internal diameter 3.2 mm). In the beginning, each reactor was inoculated using diluted overnight cultures in MM1 medium (OD_{600} ~ 0.1). After 2 hrs. stop-flow for cells' initial attachment, the MM1 medium was continuously supplied with a flow rate of 5.4 ml/hrs. for biofilm growth. After 168 hrs., the biofilms (wet biofilms) formed inside the tubular biofilm reactors were harvested and extracted onto a glass slide. Then the wet biofilms were further dried by air for 120 hrs. After totally dried, the dry biofilm samples were sent for ToF-SIMS dry sample analysis. If the samples had too much salt content, it would affect ToF-SIMS measurements due to the matrix effects. In this case, the wet samples need to be washed by DI water three times before applying the air-drying process.

The dry MM1 sample was made by dispensing a drop of liquid MM1 medium solution onto a clean glass slide or silicon wafer, followed by the freeze-drying process (-80 °C) for 120 hrs.

Supplemental Figures

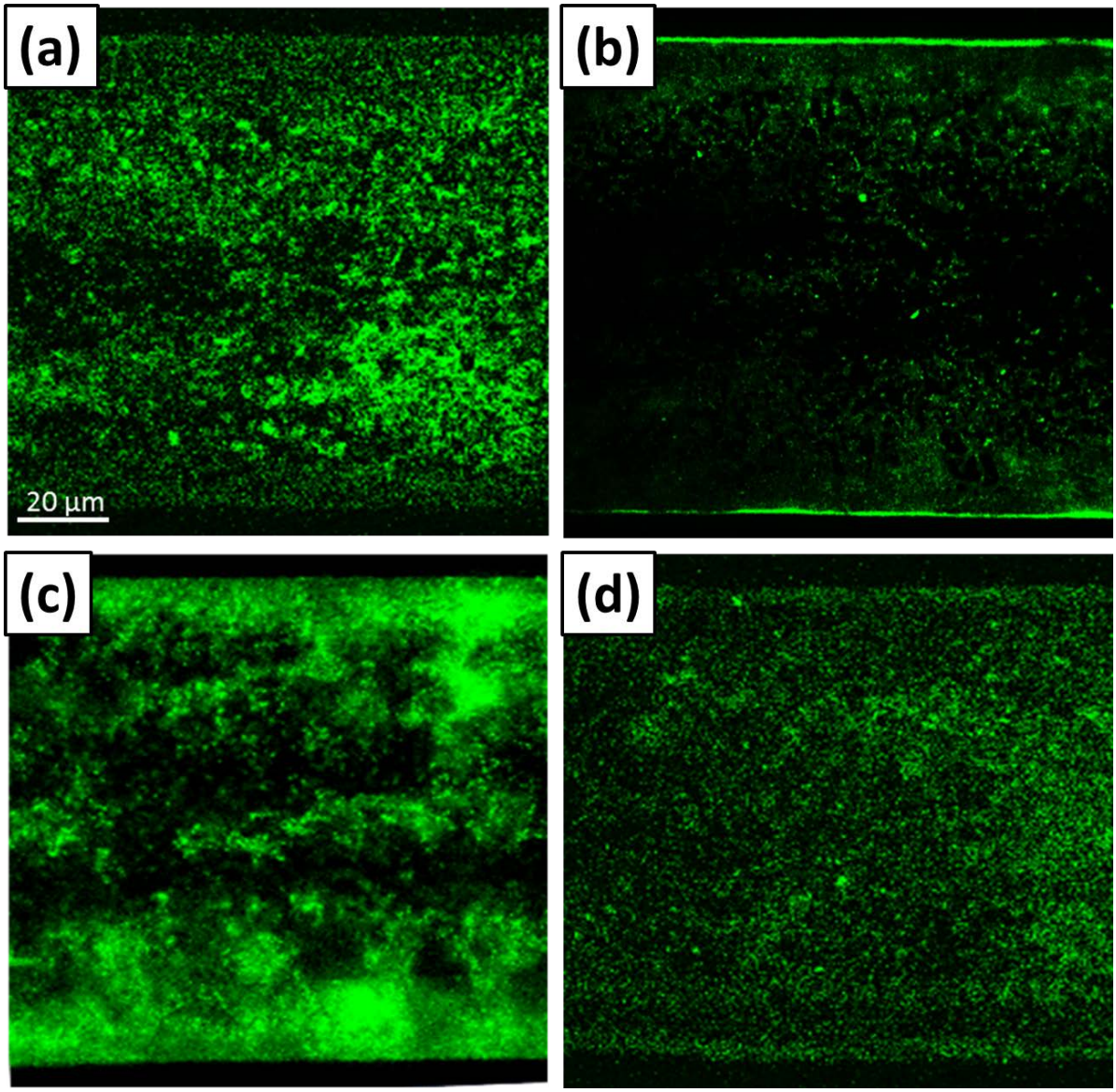

Figure S1. Fluorescence images of the biofilm in the microfluidic channels: (a) WT biofilm; (b) WT biofilm treated with Cr; (c) CP biofilm; and (d) CP biofilm treated with Cr. The white bar represents 20 µm.

The biofilms depicted above were cultured in four different SALVI devices prior to in situ liquid SIMS analysis. Therefore, the images are not comparable for each location. The comparison of fluorescence images shows the difference of the thickness of the WT and CP biofilms with and without Cr (VI) attack. In this paper, we would like to use in situ liquid SIMS to give molecular evidence and explain why the mutant CP biofilm is more resistant to toxic pollutant attacks than the WT biofilm.

i

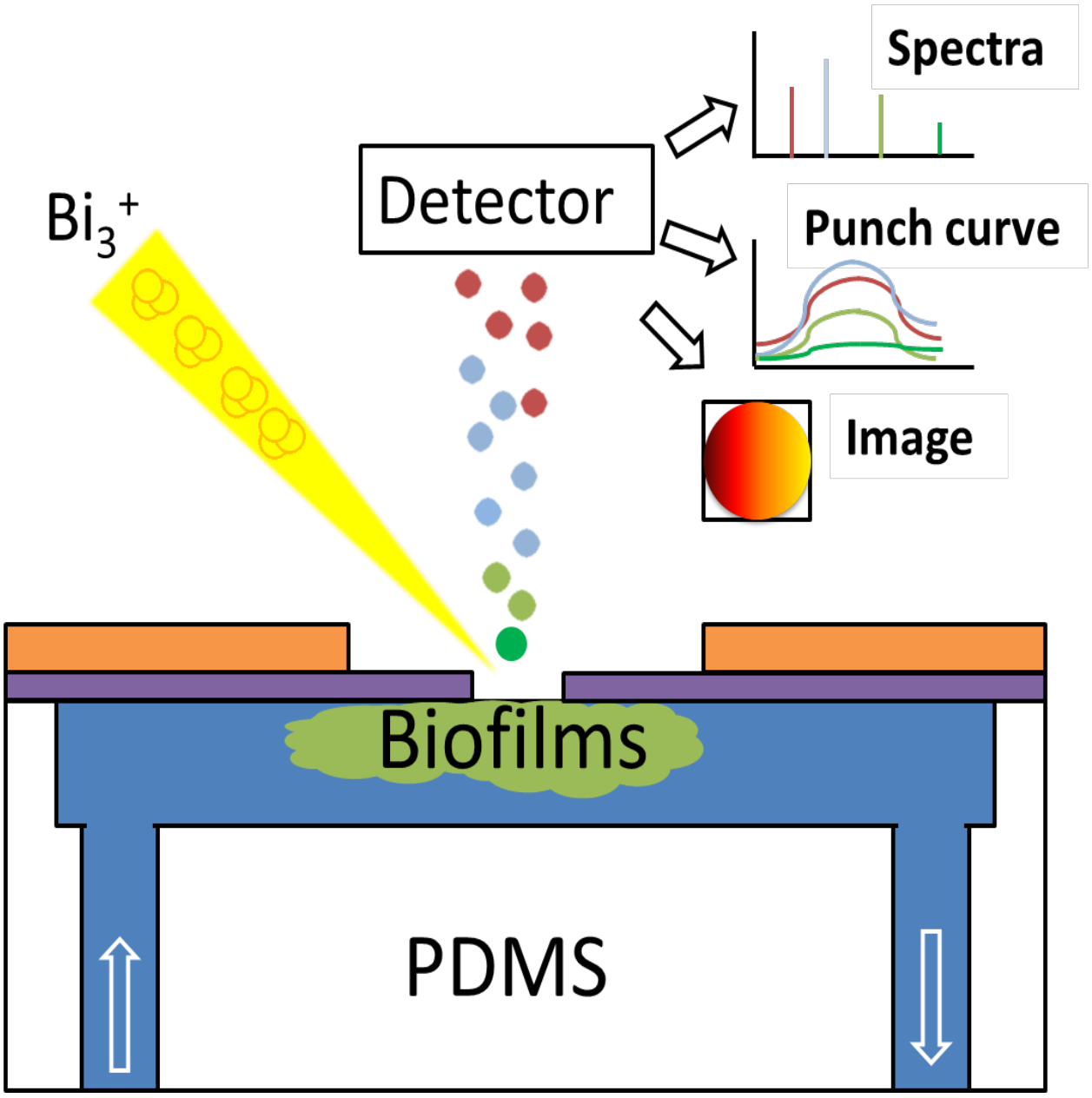

Figure S2. Schematic of the in situ liquid ToF-SIMS analysis of *S. oneidensis* MR-1 biofilms.

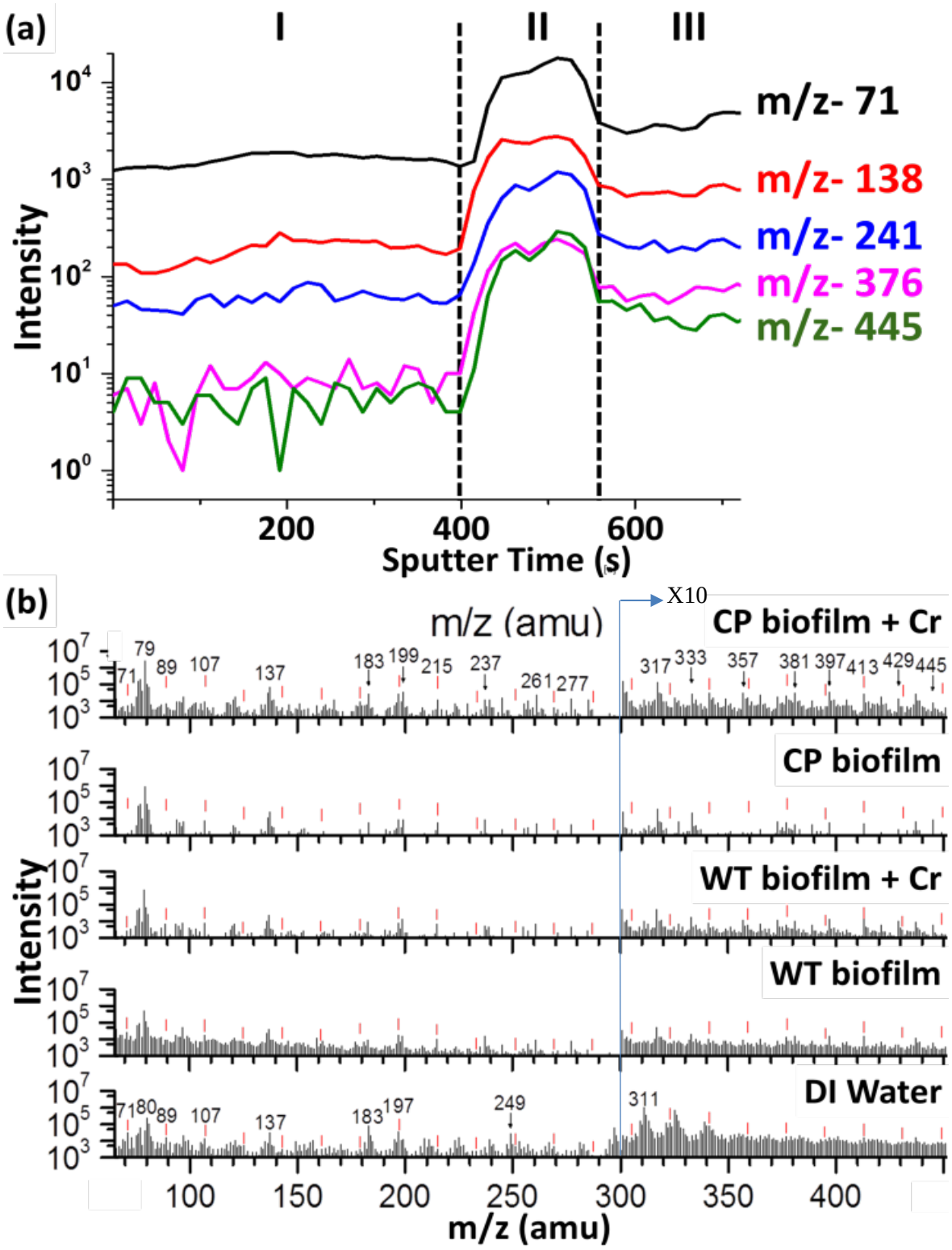

Figure S3. (a) Depth profiling of the WT biofilm in the negative mode and (b) reconstructed liquid ToF-SIMS negative spectra. Red bars depict the location of water cluster peaks.

The value is increased by 10 times in the range of m/z^+ >300 for clear observation. Additional spectra are in Figures S5 and S6.

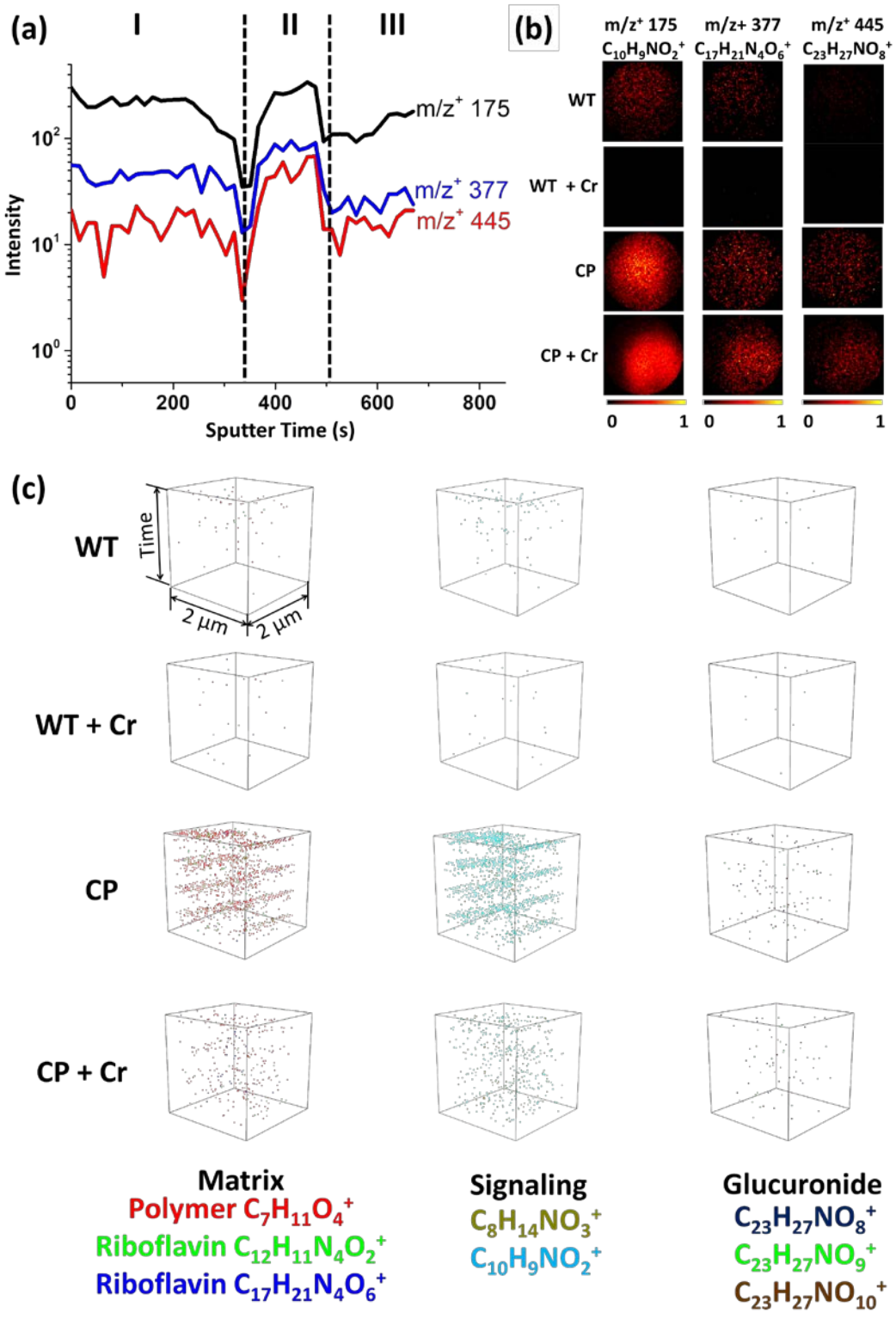

Figure S4. (a) Depth profiling of the untreated biofilm; (b) representative 2D images; (c) 3D images reconstructed from Region II in the negative depth profile.
Figure S4 provides a negative depth profile of the untreated biofilm and reconstructed represented 2D images from Region II in the depth profile time series in the positive mode. Region I: before the SiN membrane was eroded away; Region II: after the SiN membrane was eroded away; Region III: a narrower pulse width with lower current.

Figure S5 provides the m/z spectra of all samples in the positive mode.

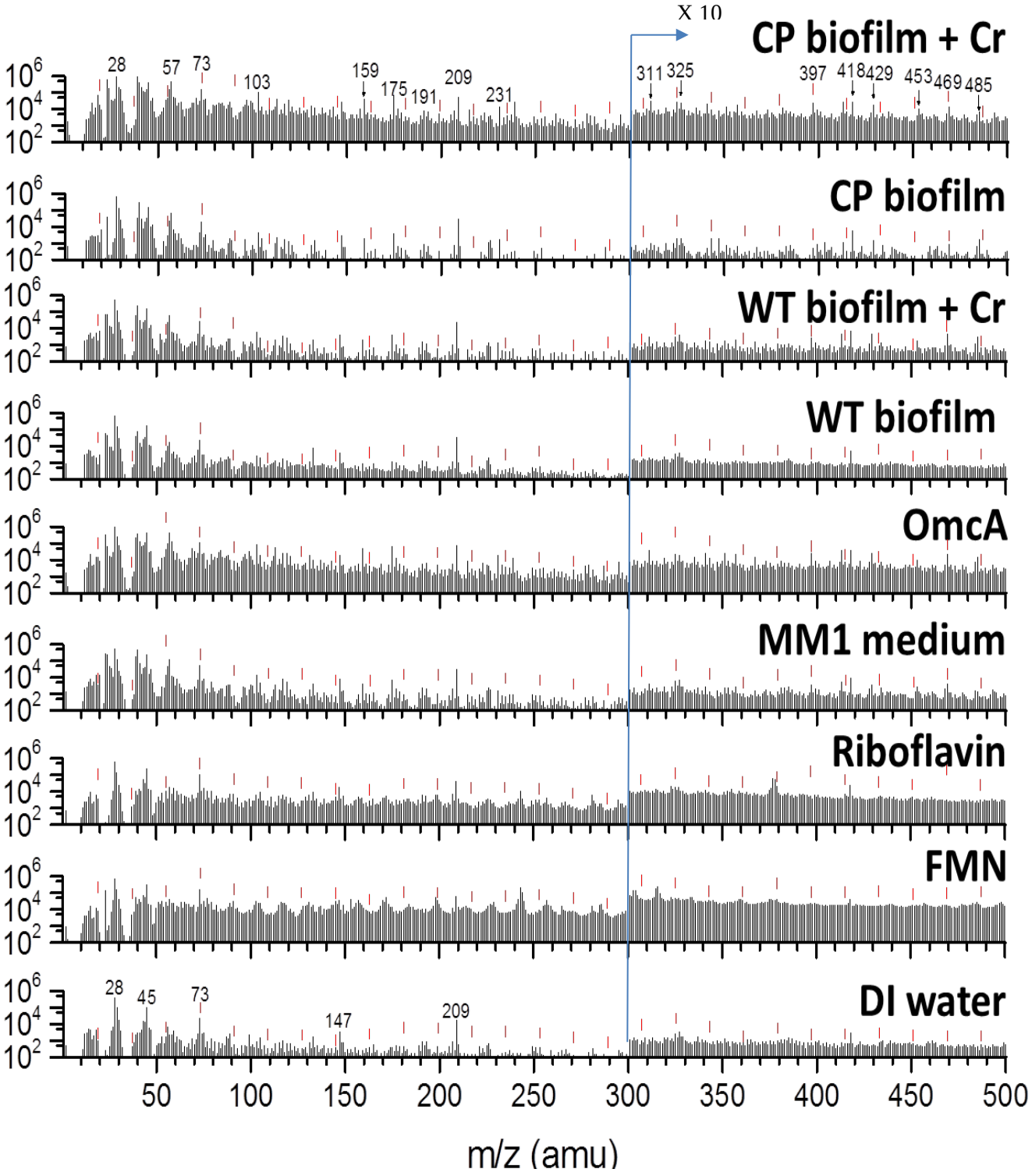

Figure S5. Liquid ToF-SIMS spectra of all samples in the positive mode. Red bars depict the location of water cluster peaks.

The value is increased by 10 times in the range of m/z^+ >300 for clear observation.

Figure S6 provides the m/z spectra of all samples in the negative mode

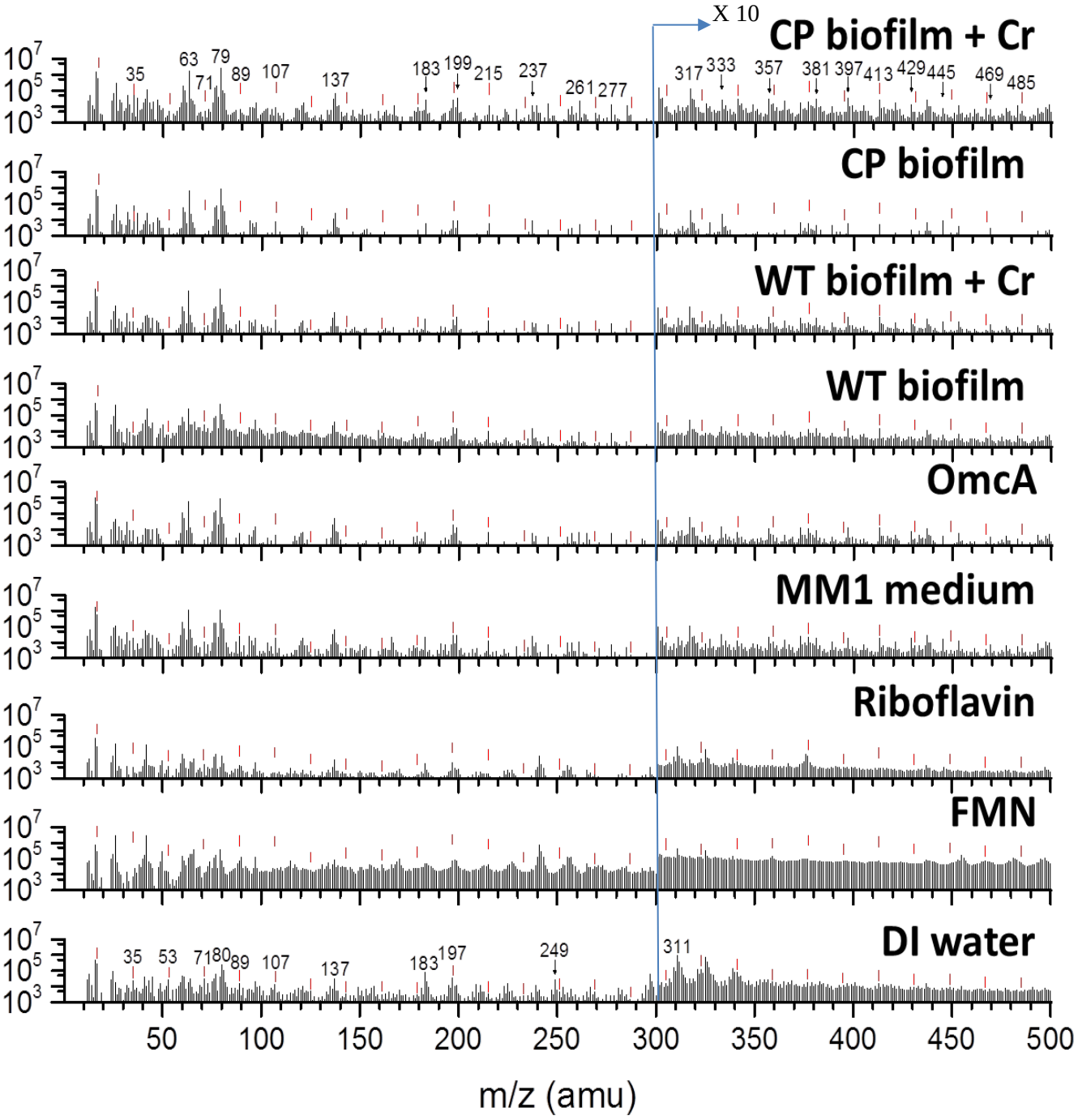

Figure S6. Liquid ToF-SIMS spectra of all samples in the negative mode. Red bars depict the location of water cluster peaks.

The value is increased by 10 times in the range of m/z^+ >300 for clear observation.

Spectral PCA was performed. Selected peaks in the m/z$^+$ range 1 to 800 atomic mass unit (amu) were used in this analysis. **Figure S7** provides additional score plots and loading plots for the positive spectral PCA using selected peaks. The selected peak list in the positive mode is summarized in **Tables S5a** and **S5b**. **Figure S7** provides additional score plots and loading plots for the negative spectral PCA using selected peaks. The selected peak list in the negative mode is summarized in **Tables S7a** and **S7b**.

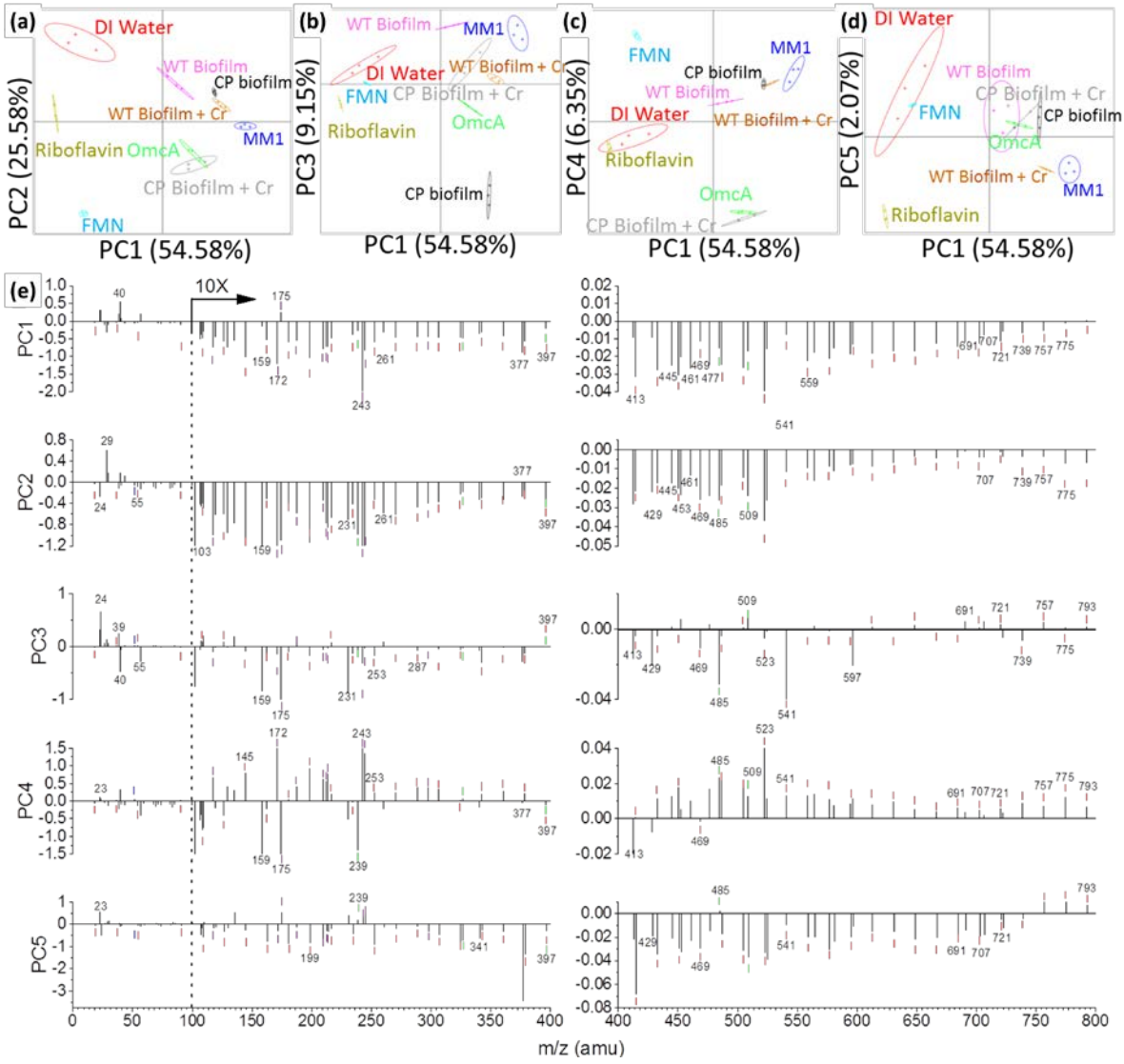

Figure S7. The scores plot of PC1 vs. PC2 (a); PC1 vs. PC3 (b); PC1 vs. PC4 (c); PC1 vs. PC4 (d) in the positively selected peaks spectral PCA. The loadings plots of each PC are depicted in (e). Red bars indicate the location of water cluster peaks, purple quorum sensing signal peaks, and green fatty acid peaks.

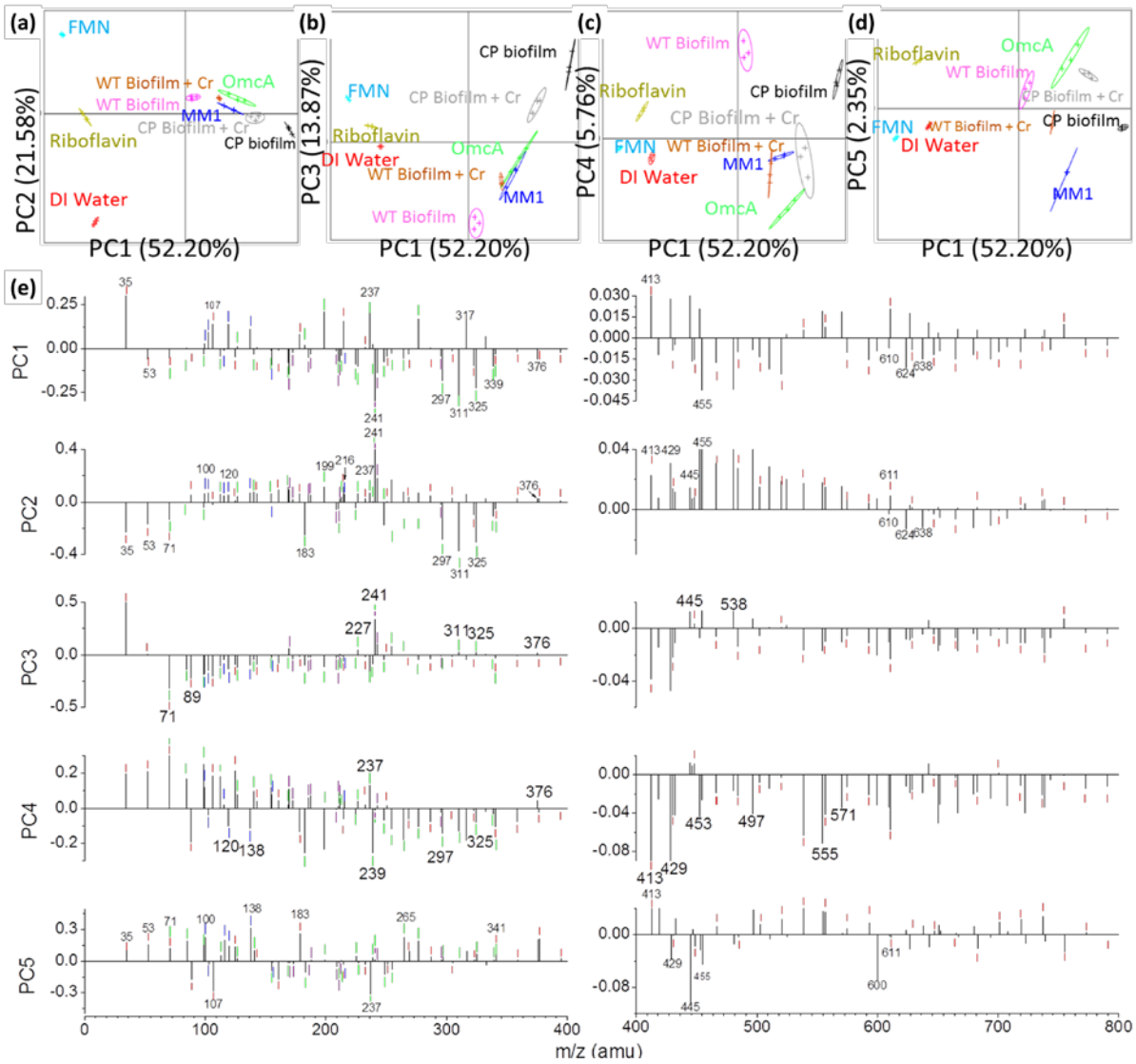

Figure S8. The scores plots of PC1 vs. PC2 (a), PC1 vs. PC3 (b), PC1-PC4 (c), and PC3-PC5 (d) in the negative selected peaks spectral PCA. The loadings plots of each PC are depicted in (e). Red bars indicate the location of water cluster peaks, blue chromium reduction related peaks, purple quorum sensing signal peaks, and green fatty acid peaks.

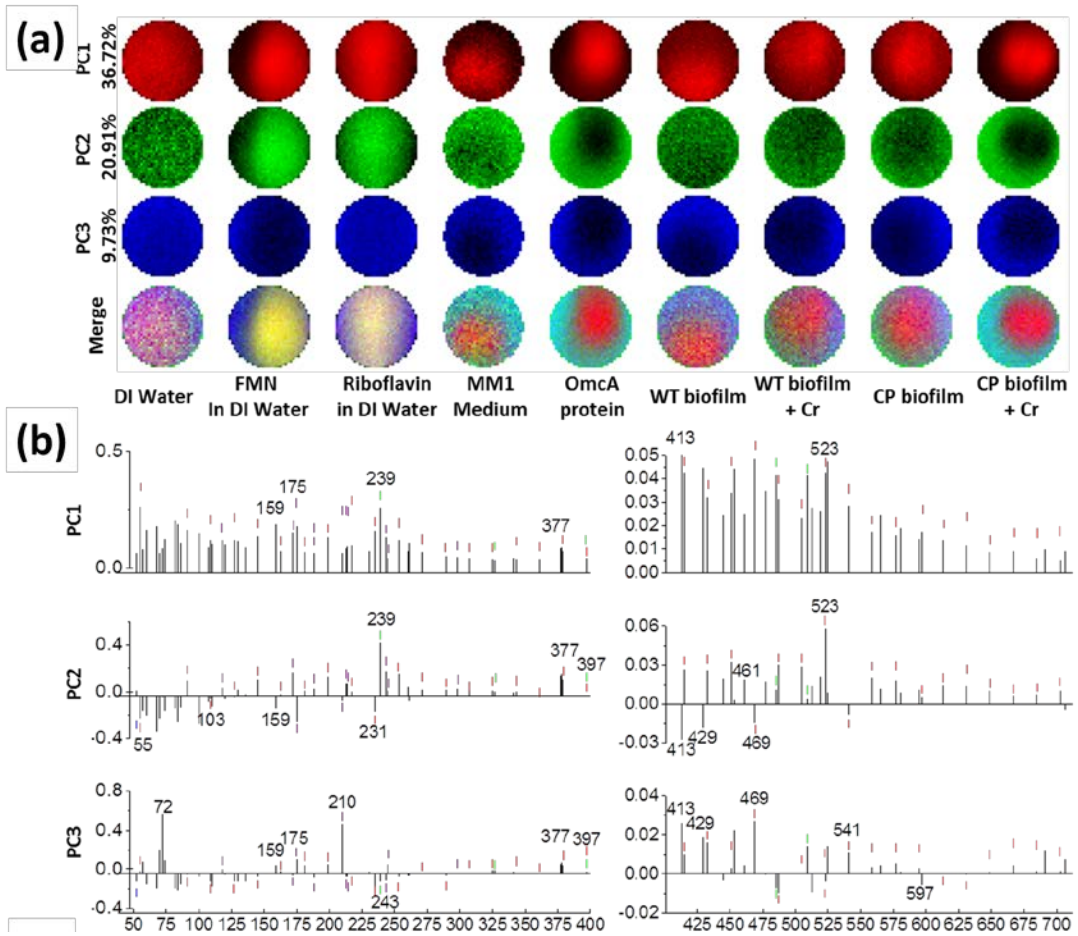

Figure S9. Image PCA in the positive ion mode. (a) Reconstructed false-color 2D PCA images in RGB corresponding to each PC scores at these locations along the microfluidic channel in the positive mode. The RGB composite images of the three key PCs are depicted. (b) Image PCA loadings plots illustrating the contribution of the selective chemical species in positive ion mode.

Only data within the 2 μm diameter circle were considered in the analysis.

Supplemental Tables

Table S1. Summary of sample descriptions

Sample	Brief name	Chemical details/ Preparation process
Shewanella oneidensis CP-2-1S1 mutant biofilm + Cr	CP+Cr/ CP2-1-S1 biofilm+Cr	Inoculate diluted overnight mutant CP2-1-S1 cultures into SALVI system. Stop the flow 4 hrs. for initial attachment. Supply MM1 medium with a flow rate of 2.88 ml/day for biofilm growth. At Day 7, add 100 µM $K_2Cr_2O_7$ into MM1 and treat the biofilms. Harvest at Day 9
Shewanella oneidensis CP-2-1S1 mutant biofilm	CP/ CP2-1-S1 biofilm	Inoculate diluted overnight mutant CP2-1-S1 cultures into SALVI system. Stop the flow 4 hrs. for initial attachment. Supply MM1 medium with a flow rate of 2.88 ml/day for biofilm growth. Harvest at Day 9.
Shewanella oneidensis MR-1 wild type (WT) biofilm + Cr	WT+Cr/WT biofilm+Cr	Inoculate diluted overnight MR-1 WT cultures into SALVI system. Stop the flow 4 hrs. for initial attachment. Supply MM1 medium with a flow rate of 2.88 ml/day for biofilm growth. At Day 7, add 100 µM $K_2Cr_2O_7$ into MM1 and treat the biofilms. Harvest at Day 9
S. oneidensis MR-1 WT biofilm*	WT/WT biofilm	Inoculate diluted overnight MR-1 WT cultures into SALVI system. Stop the flow 4 hrs. for initial attachment. Supply MM1 medium with a flow rate of 2.88 ml/day for biofilm growth. Harvest at Day 9.
S. oneidensis MR-1 Supernatant*	Supernatant	Centrifuge the planktonic cultures at 5000 g for 10 mins. Filter the supernatant by 0.22 µm membrane filter unit.
S. oneidensis MR-1 Planktonic culture*	Planktonic/Planktonic culture	Inoculate 20 µl of overnight MR-1 WT cultures into 2 ml of MM1 medium. Grow in 30 degree, 200 rpm for 24 hrs.
OmcA protein film	OmcA	Load the 100ul OmcA samples into the reservoir of centrifugal filter unit (Millipore); add buffer; Centrifuge the samples at 4000 g for 20 mins; Discard the flow through; Add 1ml MM1 medium into the reservoir of the centrifugal filter unit; Centrifuge the samples at 4000 g for 20 mins; repeat twice Collect the samples in the reservoir for ToF-SIMS experiment, and discard the flow through;
Chemically defined modified M1 medium	MM1	Contain 30.00 mM HEPES, 7.50 mM NaOH, 28.04 mM NH4Cl, 1.34 mM KCl, 4.35 mM NaH2PO4, 0.68 Mm CaCl2 supplemented with trace amounts of minerals, vitamins, and amino acids
DI water	DI water	The DI water from pure water system in Pacific Northwest National Laboratory's Biological Science Facility (BSF)

*: *Shewanella* is abbreviated as *S.*

Table S2a. Dry biofilm sample mass to charge ratios in the positive ion mode.

Unit mass	Observed m/z	Possible assignment	Theoretical m/z
23	22.99	Na^+	22.99
28	27.98	Si^+	27.98
28	28.03	$C_2H_4^+$	28.03
39	38.97	K^+	38.96
40	39.96	Ca^+	39.96
45	45.03	$C_2H_5O^+$	45.03
45	44.98	$SiOH^+$	44.98
57	57.03	$C_3H_5O^+$	57.033
57	56.97	$CaOH^+$	56.96
73	73.055	$(H_2O)_4H^+$	73.05
73	73.055	$SiC_3H_9^+$	73.05
103	103.06	$C_8H_7^+$	103.05
133	133.07	$C_4H_{13}OSi_2^+$	133.05
147	147.06	$(CH_3)_3SiOSi(CH_3)_2^+$	147.07
159	159.10	$C_6H_7O_5^+$	159.03
207	207.07	$C_5H_{15}O_3Si_3^+$	207.03
209	208.98	Bi^+	208.98
231	231.13	$C_{16}H_{23}O^+$	231.17
239	239.25	$C_{16}H_{31}O^+$	239.24
261	261.08	$C_{15}H_{11}Cl_2^+$	261.02
310	310.32	$C_{20}H_{38}O_2^+$	310.29
311	310.85	$C_{20}H_{39}O_2^+$	311.29
325	324.84	$C_{21}H_{41}O_2^+$	325.31
327	327.08	$C_{22}H_{31}O_2^+$	327.23
341	340.77	$C_{19}H_{17}O_6^+$	341.10
351	350.81	$C_{19}H_{27}O_6^+$	351.18
367	367.30	$C_{19}H_{27}O_7^+$	367.18
381	380.88	$C_{20}H_{29}O_7^+$	381.19
397	397.23	$C_{20}H_{29}O_8^+$	397.19
418	[a]	Bi_2^+	417.96
429	429.30	$C_{29}H_{49}O_2^+$	429.37
445	445.19	$C_{23}H_{27}NO_8^+$	445.17
453	453.13	$C_{28}H_{21}MgN_4O^+$	453.16
461	461.10	$C_{23}H_{27}NO_9^+$	461.17
469	469.12	$C_{28}H_{21}MgN_4O_2^+$	469.15
477	476.31	$C_{23}H_{27}NO_{10}^+$	477.16
485	485.04	$C_{28}H_{21}MgN_4O_3^+$	485.15
509	508.69	$C_{30}H_{21}MgN_4O_3^+$	509.15
541	541.33	$C_{35}H_{57}O_4^+$	541.43
565	565.35	$C_{37}H_{57}O_4^+$	565.43
597	597.35	$C_{39}H_{65}O_4^+$	597.49
627	[a]	Bi_3^+	626.94
643	[a]	Bi_3O^+	642.94
659	[a]	$Bi_3O_2^+$	658.93
691	691.55	$C_{43}H_{87}O_4Na^+$	690.65
707	707.61	$C_{43}H_{87}O_5Na^+$	706.64
723	722.497	$C_{43}H_{87}O_6Na^+$	722.64

[a]: No m/z peaks were observed in the dry biofilm sample.

Table S2b. Dry biofilm sample observed mass to charge ratios in the negative ion mode.

Unit mass m/z	Observed m/z	Possible assignment	Theoretical m/z
26	26.01	CN^-	26.00
42	42.00	CNO^-	42.00
63	62.97	PO_2^-	62.96
79	78.96	PO_3^-	78.96
137	136.92	$Si_2O_5H^-$	136.94
225	225.19	$C_2H_3(CH_2)_{11}COO^-$	225.19
237	237.21	$C_{16}H_{29}O^-$	237.22
239	239.21	$C_{16}H_{31}O^-$	239.24
255	255.23	$C_{16}H_{31}O_2^-$	255.23
277	277.07	$C_{18}H_{29}O_2^-$	277.22
297	297.15	$C_{19}H_{37}O_2^-$	297.28
311	311.21	$C_{20}H_{39}O_2^-$	311.30
325	324.07	$C_{21}H_{41}O_2^-$	325.31
339	338.83	$C_{22}H_{43}O_2^-$	339.33
341	341.05	$C_{19}H_{17}O_6^-$	341.10
381	380.79	$C_{20}H_{29}O_7^-$	381.19
421	421.14	$C_{21}H_{29}N_2O_7^-$	421.20
429	428.72	$C_{29}H_{49}O_2^-$	429.37
507	506.98	$C_{31}H_{23}MgN_4O_2^-$	507.17
539	539.07	$C_{32}H_{27}MgN_4O_3^-$	539.19
600	[a]	$C_{39}H_{67}O_4^-$	599.50
610	610.21	$C_{40}H_{66}O_4^-$	610.50
611	611.11	$C_{35}H_{31}MgN_4O_5^-$	611.22

[a]: No m/z peaks were observed in the dry biofilm sample.

Table S3a. Dry MM1 medium sample observed mass to charge ratios in the positive ion mode.

Unit mass m/z	Observed m/z	Possible assignment	Theoretical m/z
23	22.99	Na^+	22.99
28	27.98	Si^+	27.98
39	38.97	K^+	38.96
40	39.96	Ca^+	39.96
45	44.98	$SiOH^+$	44.98
57	56.97	$CaOH^+$	56.96
73	73.05	$SiC_3H_9^+$	73.05
133	133.07	$C_4H_{13}OSi_2^+$	133.05
147	147.06	$(CH_3)_3SiOSi(CH_3)_2^+$	147.07
207	207.07	$C_5H_{15}O_3Si_3^+$	207.03
209	208.98	Bi^+	208.98
418	[a]	Bi_2^+	417.96
627	[a]	Bi_3^+	626.94

[a]: No m/z peaks were observed in the dry biofilm sample.

Table S3b. Dry MM1 medium sample observed mass to charge ratios in the negative ion mode.

Unit mass m/z	Observed m/z	Possible assignment	Theoretical m/z
26	26.01	CN^-	26.00
42	42.00	CNO^-	42.00
63	62.97	PO_2^-	62.96
79	78.96	PO_3^-	78.96
137	136.92	$Si_2O_5H^-$	136.94

Table S4a. List of peaks selected in the positive spectral PCA excluding no water cluster peaks.

m/z	Peak assignment	Descriptions and notes	Reference
23	Na^+	Na^+	1
24	Mg^+	Mg^+	2
27	$C_2H_3^+$	Polysaccharides	3
29	$C_2H_5^+$	Polysaccharides	3
30	CH_4N^+	Glycine	4, 5
39	K^+	K^+	1
40	Ca^+	Ca^+	6
41	$C_3H_5^+$	Polysaccharides	3
44	$C_2H_6N^+$	Alanine	4, 5
52	Cr^+	Cr	7
55	$C_4H_7^+$	Polysaccharides	3
60	$C_2H_6NO^+$	Serine	4, 5
68	$C_4H_6N^+$	Proline	4, 5
70	$C_4H_8N^+$	Proline	4, 5
72	$C_4H_{10}N^+$	Valine	4, 5
74	$C_3H_8NO^+$	Threonine	4, 5
82	$C_4H_6N_2^+$	Histidine	4, 5
84	$C_5H_{10}N^+$	Lysine	4, 5
86	$C_4H_8NO^+/C_5H_{12}N^+$	Hydroxyproline/Leucine	4, 5
100	$C_4H_{10}N_3^+$	Arginine	4, 5
107	$C_7H_7O^+$	Tyrosine	4, 5
110	$C_5H_8N_3^+$	Histidine	4, 5
118	$C_8H_8N^+$	Indole	8
120	$C_8H_{10}N^+$	Phenylalanine	4, 5
130	$C_9H_8N^+$	Tryptophan	4, 5
136	$C_8H_{10}NO^+$	Tyrosine	4, 5
159	$C_7H_{11}O_4^+/C_6H_7O_5^+$	Polymer/Protein/Fragment of β-D-Ethyl glucuronide	9, 10
172[d]	$C_8H_{14}NO_3^+$	N-Acylhomoserine lactones (signal related)	11, 12
175[d]	$C_{10}H_9NO_2^+$	Hormones/ Quinolone signal (QS) related/ L-arginine	13-15
188[d]	$C_{11}H_{10}NO_2^+/C_8H_{14}NO_4^+$	Hormones/ Quinolone signal (QS) related/ N-Acylhomoserine lactones (signal related)	13-15
199	$C_{12}H_{23}O_2^+$	Diffusible signal factor family(DSF)	16, 17
210	$C_{11}H_{18}N_2O_2^+$	Diketopiperazines (DKPs), Cyclo (L-Leu-L-Val)	17
213	$C_{13}H_{25}O_2^+$	Diffusible signal factor family(DSF)	16, 17
214	$C_{10}H_{16}NO_4^+$	N-Acylhomoserine lactones (signal related)	11
239[d]	$C_{16}H_{31}O^+$	Palmitic acid	18, 19
243[d]	$C_{12}H_{11}N_4O_2^+$ /$C_{13}H_{23}O_4^+/C_{15}H_{31}O_2^+$	Riboflavin (loss of ribityl side chain)/A-factor (Signal related)/Diffusible signal factor family(DSF)	20-22
245	$C_{14}H_{17}N_2O_2^+$	Diketopiperazines (DKPs), Cyclo (L-Phe-L-Pro)	17
257[d]	$C_{16}H_{33}O_2^+$	Palmitic acid	18, 19
260[d]	$C_{16}H_{22}NO_2^+$	Quinolone signal (QS) related	13-15
261	$C_{15}H_{11}Cl_2^+$	Chlorine-containing polymers	23
298	$C_{16}H_{28}NO_4^+$	N-Acylhomoserine lactones (signal related)	17
327	$C_{21}H_{27}O_3^+$	Fatty acid/ Microbial mat(monoacylglycerol)	24, 25
341	$C_{19}H_{17}O_6^+$	polymers	26
343[d]	$C_{16}H_{27}N_2O_6^+$	N-Acylhomoserine lactones (signal related)	11, 12
377[d]	$C_{17}H_{21}N_4O_6^+$	Riboflavin	20-22
378[d]	$C_{17}H_{22}N_4O_6^+$	Riboflavin	20-22
397	$C_{29}H_{49}^+$	Fatty acid side chain/ Cyclic lipid (from 17α(H),21β(H)-Norhopane)	24, 25
413	$C_{28}H_{45}O_2^+$	Cyclic lipid (from α-Tocopherol)	24, 25
429	$C_{29}H_{49}O_2^+$	Cyclic lipid (from α-Tocopherol)	24, 25
445	$C_{23}H_{27}NO_8^+$	Glucuronides	27

453	$C_{18}H_{30}N_4O_8Na^+$/ $C_{28}H_{21}MgN_4O^+$	Polymer/Cyclic lipid (from Chlorophyll a)	24, 25
461	$C_{23}H_{27}NO_9^+$	Glucuronides	27
469	$C_{28}H_{21}MgN_4O_2^+$	Cyclic lipid (from Chlorophyll a)	24, 25
477	$C_{23}H_{27}NO_{10}^+$	Glucuronides	27
485	$C_{28}H_{21}MgN_4O_3^+$	Cyclic lipid (from Chlorophyll a)	24, 25
509	$C_{32}H_{61}O_4^+$	Microbial mat (diacylglycerol)	24, 25
513[d]	$C_{32}H_{65}O_4^+$	Palmitic acid	18
519[d]	$C_{32}H_{43}N_2O_4^+$	Quinolone signal (QS) related	13-15
525	$C_{34}H_{53}O_4^+$	Microbial mat (diacylglycerol)	24, 25
541	$C_{35}H_{57}O_4^+$	Microbial mat (diacylglycerol)	24, 25
566	$C_{36}H_{69}O_4^+$	Microbial mat (diacylglycerol)	24, 25
581	$C_{38}H_{61}O_4^+$	Microbial mat (diacylglycerol)	24, 25
597	$C_{39}H_{65}O_4^+$	Microbial mat (diacylglycerol)	24, 25
691	$C_{43}H_{87}O_4$+Na^+	Glycerolipids; Hydroxyarchaeol	28
707	$C_{43}H_{87}O_5$+Na^+	Glycerolipids; Hydroxyarchaeol	28
723	$C_{43}H_{87}O_6$+Na^+	Glycerolipids; Hydroxyarchaeol	28

[d]: The peaks were also identified by dry control samples, and the details were shown in the supplemental information in the previous work [29]

Table S4b. List of water cluster peaks selected in the positive spectral PCA.

m/z	Formula	Descriptions	Reference
19	$(H_2O)H^+$	Water cluster	[30-33]
37	$(H_2O)_2H^+$		
55	$(H_2O)_3H^+$		
73	$(H_2O)_4H^+$		
91	$(H_2O)_5H^+$		
109	$(H_2O)_6H^+$		
127	$(H_2O)_7H^+$		
145	$(H_2O)_8H^+$		
163	$(H_2O)_9H^+$		
181	$(H_2O)_{10}H^+$		
199	$(H_2O)_{11}H^+$		
217	$(H_2O)_{12}H^+$		
235	$(H_2O)_{13}H^+$		
253	$(H_2O)_{14}H^+$		
271	$(H_2O)_{15}H^+$		
289	$(H_2O)_{16}H^+$		
307	$(H_2O)_{17}H^+$		
325	$(H_2O)_{18}H^+$		
343	$(H_2O)_{19}H^+$		
361	$(H_2O)_{20}H^+$		
379	$(H_2O)_{21}H^+$		
397	$(H_2O)_{22}H^+$		
415	$(H_2O)_{23}H^+$		
433	$(H_2O)_{24}H^+$		
451	$(H_2O)_{25}H^+$		
469	$(H_2O)_{26}H^+$		
487	$(H_2O)_{27}H^+$		
505	$(H_2O)_{28}H^+$		
523	$(H_2O)_{29}H^+$		
541	$(H_2O)_{30}H^+$		
559	$(H_2O)_{31}H^+$		
577	$(H_2O)_{32}H^+$		
595	$(H_2O)_{33}H^+$		
613	$(H_2O)_{34}H^+$		
631	$(H_2O)_{35}H^+$		
649	$(H_2O)_{36}H^+$		
667	$(H_2O)_{37}H^+$		
685	$(H_2O)_{38}H^+$		
703	$(H_2O)_{39}H^+$		
721	$(H_2O)_{40}H^+$		
739	$(H_2O)_{41}H^+$		
757	$(H_2O)_{42}H^+$		
775	$(H_2O)_{43}H^+$		
793	$(H_2O)_{44}H^+$		

Table S5a. List of peaks selected in the negative spectral PCA (non-water cluster).

m/z	Tentative Formula	Description/Notes	Reference
71	$[C_2H_3COO]^-$	Aliphatic chain fragment ions of fatty acids	34
85	$[C_2H_3(CH_2)_1COO]^-$	Aliphatic chain fragment ions of fatty acids	34
99	$[C_2H_3(CH_2)_2COO]^-$	Aliphatic chain fragment ions of fatty acids	34
100	CrO_3^-	Cr related peak	35
103	$Cr(OH)_3^-$	Cr related peak	35
113	$[C_2H_3(CH_2)_3COO]^-$	Aliphatic chain fragment ions of fatty acids	34
116	$C_8H_6N^-/CrO_4^-$	Indole/Cr related peak	35
120	$Cr(OH)_3(s) + OH^-$	Cr related peak	35
127	$[C_2H_3(CH_2)_4COO]^-$	Aliphatic chain fragment ions of fatty acids	34
138	$Cr(OH)_3.H_2O.OH^-$	Cr related peak	35
141	$[C_2H_3(CH_2)_5COO]^-$	Aliphatic chain fragment ions of fatty acids	34
155	$[C_2H_3(CH_2)_6COO]^-$	Aliphatic chain fragment ions of fatty acids	34
156	$Cr(OH)_3.2H_2O.OH^-$	Cr related peak	35
169	$[C_2H_3(CH_2)_7COO]^-$	Aliphatic chain fragment ions of fatty acids	34
170[e]	$C_8H_{12}NO_3^-$	N-Acylhomoserine lactones (signal related)	11, 12
173[e]	$C_{10}H_7NO_2^-$	Hormones/ Quinolone signal (QS) related	13-15
183	$[C_2H_3(CH_2)_8COO]^-$	Aliphatic chain fragment ions of fatty acids	34
186[e]	$C_8H_{12}NO_4^-$ /$C_{11}H_8NO_2^-$	Hormones/ Quinolone signal (QS) related/ N-Acylhomoserine lactones (signal related)	13-15
199	$C_{12}H_{23}O_2^-$	Lauric acid	36
209	$C_{11}H_{17}N_2O_2^-$	Diketopiperazines (DKPs), Cyclo (L-Leu-L-Val)	16, 17
211	$[C_2H_3(CH_2)_{10}COO]^-$ /$C_{13}H_{23}O_2^-$	Aliphatic chain fragment ions of fatty acids/ Diffusible signal factor family(DSF)	16, 17
212	$C_{10}H_{14}NO_4^-$	N-Acylhomoserine lactones (signal related)	11
213	$CH_3(CH_2)_{11}COO^-$	Tridecylic acid	36
216	$Cr_2O_7^-$	Cr related peak	35
225	$[C_2H_3(CH_2)_{11}COO]^-$	Aliphatic chain fragment ions of fatty acids	34
227	$C_{14}H_{27}O_2^-$	Myristic acid	36
237[e]	$C_{16}H_{29}O^-$	Palmitic acid	18, 19
239	$[C_2H_3(CH_2)_{12}COO]^-$	Aliphatic chain fragment ions of fatty acids	34
241[e]	$C_{12}H_9N_4O_2^-$ /$C_{13}H_{21}O_4^-$ /$C_{15}H_{29}O_2^-$	Pentadecylic acid/Riboflavin/A-factor (Signal related)/ Diffusible signal factor family(DSF)	16, 17, 20-22, 36
243	$C_{14}H_{15}N_2O_2^-$	Diketopiperazines (DKPs), Cyclo (L-Phe-L-Pro)	16, 17
249	$C_{16}H_{25}O_2^-$	Fatty acid	24, 25
255[e]	$C_{16}H_{31}O_2^-$	Palmitic acid/Fatty acid	18, 19, 36
258[e]	$C_{16}H_{20}NO_2^-$	Hormones/ Quinolone signal (QS) related	13-15
265	$C_{17}H_{29}O_2^-$	Fatty acid	24, 25
277	$C_{18}H_{29}O_2^-$	Fatty acid	24, 25, 37
296	$C_{16}H_{26}NO_4^-$	N-Acylhomoserine lactones (signal related)	11
297	$C_{19}H_{37}O_2^-$	Fatty acid/ polar compounds	38, 39
311	$C_{20}H_{39}O_2^-$	Fatty acid/ polar compounds	38, 39
317	$C_{21}H_{33}O_2^-$	Polymer, lipids or protein related peaks	24, 25, 40
325	$C_{21}H_{41}O_2^-$	Fatty acid/ polar compounds	38, 39
333	$C_{21}H_{33}O_3^-$	Microbial mat (monoacylglycerol)	24, 25
339	$C_{22}H_{43}O_2^-$	Fatty acid/ polar compounds	38, 39
341[e]	$C_{16}H_{25}N_2O_6^-$ /$C_{21}H_{41}O_3^-$	N-Acylhomoserine lactones (signal related)/Fatty acid/polymer	11, 12
376[e]	$C_{17}H_{20}N_4O_6^-$	Riboflavin	20-22
377[e]	$C_{17}H_{21}N_4O_6^-$	Riboflavin	20-22
419	$C_{29}H_{39}O_2^-$	Cyclic lipid (from α-Tocopherol)	24, 25
429	$C_{29}H_{49}O_2^-$	Cyclic lipid (from α-Tocopherol)	24, 25
433	$C_{32}H_{49}^-$	Cyclic lipid (from β-β-Carotene)	24, 25
445	$C_{33}H_{49}^-$	Cyclic lipid (from β-β-Carotene)	24, 25
447	$C_{33}H_{51}^-$	Cyclic lipid (from β-β-Carotene)	24, 25

453	$C_{28}H_{21}MgN_4O^-$	Cyclic lipid (from Chlorophyll a)	24, 25
455	$C_{17}H_{20}N_4O_9P^-$	Flavin mononucleotide (FMN)	41
481	$C_{30}H_{25}MgN_4O^-$	Cyclic lipid (from Chlorophyll a)	24, 25
497	$C_{30}H_{25}MgN_4O_2^-$	Cyclic lipid (from Chlorophyll a)	24, 25
511[e]	$C_{32}H_{63}O_4^-/C_{33}H_{51}O_4^-$	Palmitic acid/Microbial mat (diacylglycerol)	18
517[e]	$C_{32}H_{41}N_2O_4^-$	Hormones/ Quinolone signal (QS) related	13-15
525	$C_{34}H_{53}O_4^-$	Microbial mat (diacylglycerol)	24, 25
555	$C_{36}H_{59}O_4^-$	Microbial mat (diacylglycerol)	24, 25
571	$C_{37}H_{63}O_4^-$	Microbial mat (diacylglycerol)	24, 25
601	$C_{39}H_{68}O_4^-$	Microbial mat (diacylglycerol)	24, 25
610	$C_{40}H_{66}O_4^-$	Microbial mat (diacylglycerol)	24, 25
611	$C_{35}H_{31}MgN_4O_5^-$	Cyclic lipid (from Chlorophyll a)	24, 25
625	$C_{41}H_{68}O_4^-$	Microbial mat (diacylglycerol)	24, 25
627	$C_{35}H_{31}MgN_4O_6^-$	Cyclic lipid (from Chlorophyll a)	24, 25
638	$C_{41}H_{50}O_6^-$	Microbial mat (carotenoids)	24, 25
643	$C_{41}H_{55}O_6^-$	Microbial mat (carotenoids)	24, 25
651	$C_{42}H_{51}O_6^-$	Microbial mat (carotenoids)	24, 25
652	$C_{42}H_{52}O_6^-$	Microbial mat (carotenoids)	24, 25
667	$C_{43}H_{55}O_6^-$	Microbial mat (carotenoids)	24, 25
680	$C_{44}H_{56}O_6^-$	Microbial mat (carotenoids)	24, 25
683	$C_{44}H_{59}O_6^-$	Microbial mat (carotenoids)	24, 25
694	$C_{45}H_{58}O_6^-$	Microbial mat (carotenoids)	24, 25
708	$C_{46}H_{60}O_6^-$	Microbial mat (carotenoids)	24, 25
723	$C_{47}H_{63}O_6^-$	Microbial mat (carotenoids)	24, 25
739	$C_{48}H_{67}O_6^-$	Microbial mat (triacylglycerol)	24, 25
744	$C_{48}H_{71}O_6^-$	Microbial mat (triacylglycerol)	24, 25
755	$C_{49}H_{70}O_6^-$	Microbial mat (triacylglycerol)	24, 25

[e]: The peaks were also identified by dry control samples, and the details were shown in the supplemental information in the previous work [29]

Table S5b. List of peaks selected in the negative spectral PCA (water cluster).

Mass/Charge	Formula	Descriptions	Reference
17	OH^-	Water cluster	[30-33]
35	H_2OOH^-		
53	$(H_2O)_2OH^-$		
71	$(H_2O)_3OH^-$		
89	$(H_2O)_4OH^-$		
107	$(H_2O)_5OH^-$		
125	$(H_2O)_6OH^-$		
143	$(H_2O)_7OH^-$		
161	$(H_2O)_8OH^-$		
179	$(H_2O)_9OH^-$		
215	$(H_2O)_{11}OH^-$		
233	$(H_2O)_{12}OH^-$		
251	$(H_2O)_{13}OH^-$		
269	$(H_2O)_{14}OH^-$		
287	$(H_2O)_{15}OH^-$		
305	$(H_2O)_{16}OH^-$		
323	$(H_2O)_{17}OH^-$		
341	$(H_2O)_{18}OH^-$		
359	$(H_2O)_{19}OH^-$		
377	$(H_2O)_{20}OH^-$		
395	$(H_2O)_{21}OH^-$		
413	$(H_2O)_{22}OH^-$		
431	$(H_2O)_{23}OH^-$		
449	$(H_2O)_{24}OH^-$		
467	$(H_2O)_{25}OH^-$		
485	$(H_2O)_{26}OH^-$		
503	$(H_2O)_{27}OH^-$		
521	$(H_2O)_{28}OH^-$		
539	$(H_2O)_{29}OH^-$		
557	$(H_2O)_{30}OH^-$		
575	$(H_2O)_{31}OH^-$		
593	$(H_2O)_{32}OH^-$		
611	$(H_2O)_{33}OH^-$		
629	$(H_2O)_{34}OH^-$		
647	$(H_2O)_{35}OH^-$		
665	$(H_2O)_{36}OH^-$		
683	$(H_2O)_{37}OH^-$		
701	$(H_2O)_{38}OH^-$		
719	$(H_2O)_{39}OH^-$		
737	$(H_2O)_{40}OH^-$		
755	$(H_2O)_{41}OH^-$		
773	$(H_2O)_{42}OH^-$		
791	$(H_2O)_{43}OH^-$		

Table S6a. List of peaks selected in the positive 2D image PCA excluding water cluster peaks.

m/z	Peak assignment	Descriptions and notes	Reference
52	Cr^+	Cr	7
55	$C_4H_7^+$	Polysaccharides	3
60	$C_2H_6NO^+$	Serine	4, 5
68	$C_4H_6N^+$	Proline	4, 5
70	$C_4H_8N^+$	Proline	4, 5
72	$C_4H_{10}N^+$	Valine	4, 5
74	$C_3H_8NO^+$	Threonine	4, 5
82	$C_4H_6N_2^+$	Histidine	4, 5
84	$C_5H_{10}N^+$	Lysine	4, 5
86	$C_4H_8NO^+/C_5H_{12}N^+$	Hydroxyproline/Leucine	4, 5
100	$C_4H_{10}N_3^+$	Arginine	4, 5
107	$C_7H_7O^+$	Tyrosine	4, 5
110	$C_5H_8N_3^+$	Histidine	4, 5
118	$C_8H_8N^+$	Indole	8
120	$C_8H_{10}N^+$	Phenylalanine	4, 5
130	$C_9H_8N^+$	Tryptophan	4, 5
136	$C_8H_{10}NO^+$	Tyrosine	4, 5
159	$C_7H_{11}O_4^+/C_6H_7O_5^+$	Polymer/Protein/Fragment of β-D-Ethyl glucuronide	9, 10
172[d]	$C_8H_{14}NO_3^+$	N-Acylhomoserine lactones (signal related)	11, 12
175[d]	$C_{10}H_9NO_2^+$	Hormones/ Quinolone signal (QS) related/ L-arginine	13-15
188[d]	$C_{11}H_{10}NO_2^+/C_8H_{14}NO_4^+$	Hormones/ Quinolone signal (QS) related/ N-Acylhomoserine lactones (signal related)	13-15
199	$C_{12}H_{23}O_2^+$	Diffusible signal factor family(DSF)	16, 17
210	$C_{11}H_{18}N_2O_2^+$	Diketopiperazines (DKPs), Cyclo (L-Leu-L-Val)	17
213	$C_{13}H_{25}O_2^+$	Diffusible signal factor family(DSF)	16, 17
214	$C_{10}H_{16}NO_4^+$	N-Acylhomoserine lactones (signal related)	11
239[d]	$C_{16}H_{31}O^+$	Palmitic acid	18, 19
243[d]	$C_{12}H_{11}N_4O_2^+$ /$C_{13}H_{23}O_4^+/C_{15}H_{31}O_2^+$	Riboflavin (loss of ribityl side chain)/A-factor (Signal related)/Diffusible signal factor family(DSF)	20-22
245	$C_{14}H_{17}N_2O_2^+$	Diketopiperazines (DKPs), Cyclo (L-Phe-L-Pro)	17
257[d]	$C_{16}H_{33}O_2^+$	Palmitic acid	18, 19
260[d]	$C_{16}H_{22}NO_2^+$	Quinolone signal (QS) related	13-15
261	$C_{15}H_{11}Cl_2^+$	Chlorine-containing polymers	23
298	$C_{16}H_{28}NO_4^+$	N-Acylhomoserine lactones (signal related)	17
327	$C_{21}H_{27}O_3^+$	Fatty acid/ Microbial mat(monoacylglycerol)	24, 25
341	$C_{19}H_{17}O_6^+$	polymers	26
343[d]	$C_{16}H_{27}N_2O_6^+$	N-Acylhomoserine lactones (signal related)	11, 12
377[d]	$C_{17}H_{21}N_4O_6^+$	Riboflavin	20-22
378[d]	$C_{17}H_{22}N_4O_6^+$	Riboflavin	20-22
397	$C_{29}H_{49}^+$	Fatty acid side chain/ Cyclic lipid (from 17α(H),21β(H)-Norhopane)	24, 25
413	$C_{28}H_{45}O_2^+$	Cyclic lipid (from α-Tocopherol)	24, 25
429	$C_{29}H_{49}O_2^+$	Cyclic lipid (from α-Tocopherol)	24, 25
445	$C_{23}H_{27}NO_8^+$	Glucuronides	27
453	$C_{18}H_{30}N_4O_8Na^+$/ $C_{28}H_{21}MgN_4O^+$	Polymer/Cyclic lipid (from Chlorophyll a)	24, 25
461	$C_{23}H_{27}NO_9^+$	Glucuronides	27
469	$C_{28}H_{21}MgN_4O_2^+$	Cyclic lipid (from Chlorophyll a)	24, 25
477	$C_{23}H_{27}NO_{10}^+$	Glucuronides	27
485	$C_{28}H_{21}MgN_4O_3^+$	Cyclic lipid (from Chlorophyll a)	24, 25
509	$C_{32}H_{61}O_4^+$	Microbial mat (diacylglycerol)	24, 25
513[d]	$C_{32}H_{65}O_4^+$	Palmitic acid	18

519[d]	$C_{32}H_{43}N_2O_4^+$	Quinolone signal (QS) related	13-15
525	$C_{34}H_{53}O_4^+$	Microbial mat (diacylglycerol)	24, 25
541	$C_{35}H_{57}O_4^+$	Microbial mat (diacylglycerol)	24, 25
566	$C_{36}H_{69}O_4^+$	Microbial mat (diacylglycerol)	24, 25
581	$C_{38}H_{61}O_4^+$	Microbial mat (diacylglycerol)	24, 25
597	$C_{39}H_{65}O_4^+$	Microbial mat (diacylglycerol)	24, 25
691	$C_{43}H_{87}O_4+Na^+$	Glycerolipids; Hydroxyarchaeol	28
707	$C_{43}H_{87}O_5+Na^+$	Glycerolipids; Hydroxyarchaeol	28
723	$C_{43}H_{87}O_6+Na^+$	Glycerolipids; Hydroxyarchaeol	28

[d]: The peaks were also identified by dry control samples, and the details were shown in the supplemental information in the previous work [29]

Table S6b. List of water cluster peaks included in the positive 2D image PCA.

m/z	Formula	Descriptions	Reference
55	$(H_2O)_3H^+$	Water cluster	[30-33]
73	$(H_2O)_4H^+$		
91	$(H_2O)_5H^+$		
109	$(H_2O)_6H^+$		
127	$(H_2O)_7H^+$		
145	$(H_2O)_8H^+$		
163	$(H_2O)_9H^+$		
181	$(H_2O)_{10}H^+$		
199	$(H_2O)_{11}H^+$		
217	$(H_2O)_{12}H^+$		
235	$(H_2O)_{13}H^+$		
253	$(H_2O)_{14}H^+$		
271	$(H_2O)_{15}H^+$		
289	$(H_2O)_{16}H^+$		
307	$(H_2O)_{17}H^+$		
325	$(H_2O)_{18}H^+$		
343	$(H_2O)_{19}H^+$		
361	$(H_2O)_{20}H^+$		
379	$(H_2O)_{21}H^+$		
397	$(H_2O)_{22}H^+$		
415	$(H_2O)_{23}H^+$		
433	$(H_2O)_{24}H^+$		
451	$(H_2O)_{25}H^+$		
469	$(H_2O)_{26}H^+$		
487	$(H_2O)_{27}H^+$		
505	$(H_2O)_{28}H^+$		
523	$(H_2O)_{29}H^+$		
541	$(H_2O)_{30}H^+$		
559	$(H_2O)_{31}H^+$		
577	$(H_2O)_{32}H^+$		
595	$(H_2O)_{33}H^+$		
613	$(H_2O)_{34}H^+$		
631	$(H_2O)_{35}H^+$		
649	$(H_2O)_{36}H^+$		
667	$(H_2O)_{37}H^+$		
685	$(H_2O)_{38}H^+$		
703	$(H_2O)_{39}H^+$		
721	$(H_2O)_{40}H^+$		
739	$(H_2O)_{41}H^+$		
757	$(H_2O)_{42}H^+$		
775	$(H_2O)_{43}H^+$		
793	$(H_2O)_{44}H^+$		

Table S7a. List of peaks selected in the negative 2D image PCA excluding water cluster peaks.

m/z	Tentative Formula	Description/Notes	Reference
71	$[C_2H_3COO]^-$	Aliphatic chain fragment ions of fatty acids	34
85	$[C_2H_3(CH_2)_1COO]^-$	Aliphatic chain fragment ions of fatty acids	34
99	$[C_2H_3(CH_2)_2COO]^-$	Aliphatic chain fragment ions of fatty acids	34
100	CrO_3^-	Cr related peak	35
103	$Cr(OH)_3^-$	Cr related peak	35
113	$[C_2H_3(CH_2)_3COO]^-$	Aliphatic chain fragment ions of fatty acids	34
116	$C_8H_6N^-/CrO_4^-$	Indole/Cr related peak	35
120	$Cr(OH)_3(s) + OH^-$	Cr related peak	35
127	$[C_2H_3(CH_2)_4COO]^-$	Aliphatic chain fragment ions of fatty acids	34
138	$Cr(OH)_3.H_2O.OH^-$	Cr related peak	35
141	$[C_2H_3(CH_2)_5COO]^-$	Aliphatic chain fragment ions of fatty acids	34
155	$[C_2H_3(CH_2)_6COO]^-$	Aliphatic chain fragment ions of fatty acids	34
156	$Cr(OH)_3.2H_2O.OH^-$	Cr related peak	35
169	$[C_2H_3(CH_2)_7COO]^-$	Aliphatic chain fragment ions of fatty acids	34
170[e]	$C_8H_{12}NO_3^-$	N-Acylhomoserine lactones (signal related)	11, 12
173[e]	$C_{10}H_7NO_2^-$	Hormones/ Quinolone signal (QS) related	13-15
183	$[C_2H_3(CH_2)_8COO]^-$	Aliphatic chain fragment ions of fatty acids	34
186[e]	$C_8H_{12}NO_4^-$ /$C_{11}H_8NO_2^-$	Hormones/ Quinolone signal (QS) related/ N-Acylhomoserine lactones (signal related)	13-15
199	$C_{12}H_{23}O_2^-$	Lauric acid	36
209	$C_{11}H_{17}N_2O_2^-$	Diketopiperazines (DKPs), Cyclo (L-Leu-L-Val)	16, 17
211	$[C_2H_3(CH_2)_{10}COO]^-$ /$C_{13}H_{23}O_2^-$	Aliphatic chain fragment ions of fatty acids/ Diffusible signal factor family(DSF)	16, 17
212	$C_{10}H_{14}NO_4^-$	N-Acylhomoserine lactones (signal related)	11
213	$CH_3(CH_2)_{11}COO^-$	Tridecylic acid	36
216	$Cr_2O_7^-$	Cr related peak	35
225	$[C_2H_3(CH_2)_{11}COO]^-$	Aliphatic chain fragment ions of fatty acids	34
227	$C_{14}H_{27}O_2^-$	Myristic acid	36
237[e]	$C_{16}H_{29}O^-$	Palmitic acid	18, 19
239	$[C_2H_3(CH_2)_{12}COO]^-$	Aliphatic chain fragment ions of fatty acids	34
241[e]	$C_{12}H_9N_4O_2^-$ /$C_{13}H_{21}O_4^-$ /$C_{15}H_{29}O_2^-$	Pentadecylic acid/Riboflavin/A-factor (Signal related)/ Diffusible signal factor family(DSF)	16, 17, 20-22, 36
243	$C_{14}H_{15}N_2O_2^-$	Diketopiperazines (DKPs), Cyclo (L-Phe-L-Pro)	16, 17
249	$C_{16}H_{25}O_2^-$	Fatty acid	24, 25
255[e]	$C_{16}H_{31}O_2^-$	Palmitic acid/Fatty acid	18, 19, 36
258[e]	$C_{16}H_{20}NO_2^-$	Hormones/ Quinolone signal (QS) related	13-15
265	$C_{17}H_{29}O_2^-$	Fatty acid	24, 25
277	$C_{18}H_{29}O_2^-$	Fatty acid	24, 25, 37
296	$C_{16}H_{26}NO_4^-$	N-Acylhomoserine lactones (signal related)	11
297	$C_{19}H_{37}O_2^-$	Fatty acid/ polar compounds	38, 39
311	$C_{20}H_{39}O_2^-$	Fatty acid/ polar compounds	38, 39
317	$C_{21}H_{33}O_2^-$	Polymer, lipids or protein related peaks	24, 25, 40
325	$C_{21}H_{41}O_2^-$	Fatty acid/ polar compounds	38, 39
333	$C_{21}H_{33}O_3^-$	Microbial mat (monoacylglycerol)	24, 25
339	$C_{22}H_{43}O_2^-$	Fatty acid/ polar compounds	38, 39
341[e]	$C_{16}H_{25}N_2O_6^-$ /$C_{21}H_{41}O_3^-$	N-Acylhomoserine lactones (signal related)/Fatty acid/polymer	11, 12
376[e]	$C_{17}H_{20}N_4O_6^-$	Riboflavin	20-22
377[e]	$C_{17}H_{21}N_4O_6^-$	Riboflavin	20-22
419	$C_{29}H_{39}O_2^-$	Cyclic lipid (from α-Tocopherol)	24, 25
429	$C_{29}H_{49}O_2^-$	Cyclic lipid (from α-Tocopherol)	24, 25
433	$C_{32}H_{49}^-$	Cyclic lipid (from β-β-Carotene)	24, 25
445	$C_{33}H_{49}^-$	Cyclic lipid (from β-β-Carotene)	24, 25
447	$C_{33}H_{51}^-$	Cyclic lipid (from β-β-Carotene)	24, 25

453	$C_{28}H_{21}MgN_4O^-$	Cyclic lipid (from Chlorophyll a)	24, 25
455	$C_{17}H_{20}N_4O_9P^-$	Flavin mononucleotide (FMN)	41
481	$C_{30}H_{25}MgN_4O^-$	Cyclic lipid (from Chlorophyll a)	24, 25
497	$C_{30}H_{25}MgN_4O_2^-$	Cyclic lipid (from Chlorophyll a)	24, 25
511[e]	$C_{32}H_{63}O_4^-/C_{33}H_{51}O_4^-$	Palmitic acid/Microbial mat (diacylglycerol)	18
517[e]	$C_{32}H_{41}N_2O_4^-$	Hormones/ Quinolone signal (QS) related	13-15
525	$C_{34}H_{53}O_4^-$	Microbial mat (diacylglycerol)	24, 25
555	$C_{36}H_{59}O_4^-$	Microbial mat (diacylglycerol)	24, 25
571	$C_{37}H_{63}O_4^-$	Microbial mat (diacylglycerol)	24, 25
601	$C_{39}H_{68}O_4^-$	Microbial mat (diacylglycerol)	24, 25
610	$C_{40}H_{66}O_4^-$	Microbial mat (diacylglycerol)	24, 25
611	$C_{35}H_{31}MgN_4O_5^-$	Cyclic lipid (from Chlorophyll a)	24, 25
625	$C_{41}H_{68}O_4^-$	Microbial mat (diacylglycerol)	24, 25
627	$C_{35}H_{31}MgN_4O_6^-$	Cyclic lipid (from Chlorophyll a)	24, 25
638	$C_{41}H_{50}O_6^-$	Microbial mat (carotenoids)	24, 25
643	$C_{41}H_{55}O_6^-$	Microbial mat (carotenoids)	24, 25
651	$C_{42}H_{51}O_6^-$	Microbial mat (carotenoids)	24, 25
652	$C_{42}H_{52}O_6^-$	Microbial mat (carotenoids)	24, 25
667	$C_{43}H_{55}O_6^-$	Microbial mat (carotenoids)	24, 25
680	$C_{44}H_{56}O_6^-$	Microbial mat (carotenoids)	24, 25
683	$C_{44}H_{59}O_6^-$	Microbial mat (carotenoids)	24, 25
694	$C_{45}H_{58}O_6^-$	Microbial mat (carotenoids)	24, 25
708	$C_{46}H_{60}O_6^-$	Microbial mat (carotenoids)	24, 25
723	$C_{47}H_{63}O_6^-$	Microbial mat (carotenoids)	24, 25
739	$C_{48}H_{67}O_6^-$	Microbial mat (triacylglycerol)	24, 25
744	$C_{48}H_{71}O_6^-$	Microbial mat (triacylglycerol)	24, 25
755	$C_{49}H_{70}O_6^-$	Microbial mat (triacylglycerol)	24, 25

[e]: The peaks were also identified by dry control samples, and the details were shown in the supplemental information in the previous work [29]

Table S7b. List of water cluster peaks included in the negative 2D image PCA (water cluster).

Mass/Charge	Formula	Descriptions	Reference
71	$(H_2O)_3OH^-$	Water cluster	[30-33]
89	$(H_2O)_4OH^-$		
107	$(H_2O)_5OH^-$		
125	$(H_2O)_6OH^-$		
143	$(H_2O)_7OH^-$		
161	$(H_2O)_8OH^-$		
179	$(H_2O)_9OH^-$		
215	$(H_2O)_{11}OH^-$		
233	$(H_2O)_{12}OH^-$		
251	$(H_2O)_{13}OH^-$		
269	$(H_2O)_{14}OH^-$		
287	$(H_2O)_{15}OH^-$		
305	$(H_2O)_{16}OH^-$		
323	$(H_2O)_{17}OH^-$		
341	$(H_2O)_{18}OH^-$		
359	$(H_2O)_{19}OH^-$		
377	$(H_2O)_{20}OH^-$		
395	$(H_2O)_{21}OH^-$		
413	$(H_2O)_{22}OH^-$		
431	$(H_2O)_{23}OH^-$		
449	$(H_2O)_{24}OH^-$		
467	$(H_2O)_{25}OH^-$		
485	$(H_2O)_{26}OH^-$		
503	$(H_2O)_{27}OH^-$		
521	$(H_2O)_{28}OH^-$		
539	$(H_2O)_{29}OH^-$		
557	$(H_2O)_{30}OH^-$		
575	$(H_2O)_{31}OH^-$		
593	$(H_2O)_{32}OH^-$		
611	$(H_2O)_{33}OH^-$		
629	$(H_2O)_{34}OH^-$		
647	$(H_2O)_{35}OH^-$		
665	$(H_2O)_{36}OH^-$		
683	$(H_2O)_{37}OH^-$		
701	$(H_2O)_{38}OH^-$		
719	$(H_2O)_{39}OH^-$		
737	$(H_2O)_{40}OH^-$		
755	$(H_2O)_{41}OH^-$		
773	$(H_2O)_{42}OH^-$		
791	$(H_2O)_{43}OH^-$		

References

1. H. Nygren, B. Hagenhoff, P. Malmberg, M. Nilsson and K. Richter, *Microsc Res Tech*, 2007, **70**, 969-974.
2. S. Chandra, D. R. Smith and G. H. Morrison, *Analytical Chemistry*, 2000, **72**, 104a-114a.
3. S. L. McArthur, M. S. Wagner, P. G. Hartley, K. M. McLean, H. J. Griesser and D. G. Castner, *Surface and Interface Analysis*, 2002, **33**, 924-931.
4. C. Bruuning, S. Hellweg, S. Dambach, D. Lipinsky and H. F. Arlinghaus, *Surface and Interface Analysis*, 2006, **38**, 191-193.
5. B. J. Tyler, C. Bruening, S. Rangaranjan and H. F. Arlinghaus, *Biointerphases*, 2011, **6**, 135-141.
6. G. S. Groenewold, J. C. Ingram, T. McLing, A. K. Gianotto and R. Avci, *Analytical Chemistry*, 1998, **70**, 534-539.
7. N. Ali, Y. Kousar, T. I. Okpalugo, V. Singh, M. Pease, A. A. Ogwu, J. Gracio, E. Titus, E. I. Meletis and M. J. Jackson, *Thin Solid Films*, 2006, **515**, 59-65.
8. H. R. Bokesch, L. K. Pannell, T. C. McKee and M. R. Boyd, *Tetrahedron Letters*, 2000, **41**, 6305-6308.
9. J. Lahann, M. Balcells, T. Rodon, J. Lee, I. S. Choi, K. F. Jensen and R. Langer, *Langmuir*, 2002, **18**, 3632-3638.
10. B. Duretz, A. Schreiber, T. Sakuma, T. Sasaki, T. Gamble and W. Weinmann, *Therapeutic Drug Monitoring*, 2007, **29**, 498-498.
11. M. Liu, H. Wang and M. W. Griffiths, *Journal of Applied Microbiology*, 2007, **103**, 2174-2184.
12. C. Y. Chang, T. Krishnan, H. Wang, Y. Chen, W. F. Yin, Y. M. Chong, L. Y. Tan, T. M. Chong and K. G. Chan, *Scientific Reports*, 2014, **4**.
13. E. J. Lanni, R. N. Masyuko, C. M. Driscoll, J. T. Aerts, J. D. Shrout, P. W. Bohn and J. V. Sweedler, *Analytical Chemistry*, 2014, **86**, 9139-9145.
14. F. Lepine, S. Milot, E. Deziel, J. X. He and L. G. Rahme, *Journal of the American Society for Mass Spectrometry*, 2004, **15**, 862-869.
15. E. J. Lanni, R. N. Masyuko, C. M. Driscoll, S. J. B. Dunham, J. D. Shrout, P. W. Bohn and J. V. Sweedler, *Analytical Chemistry*, 2014, **86**, 10885-10891.
16. K. B. Twomey, O. J. O'Connell, Y. McCarthy, J. M. Dow, G. A. O'Toole, B. J. Plant and R. P. Ryan, *Isme Journal*, 2012, **6**, 939-950.
17. R. P. Ryan and J. M. Dow, *Microbiology-Sgm*, 2008, **154**, 1845-1858.
18. T. M. Kuo, L. K. Manthey and C. T. Hou, *Journal of the American Oil Chemists Society*, 1998, **75**, 875-879.
19. H. L. Wang, O. Brattstrom, P. M. Brakefield, W. Francke and C. Lofstedt, *Journal of Chemical Ecology*, 2014, **40**, 549-559.
20. E. Marsili, D. B. Baron, I. D. Shikhare, D. Coursolle, J. A. Gralnick and D. R. Bond, *Proceedings of the National Academy of Sciences of the United States of America*, 2008, **105**, 3968-3973.
21. D. Uyakul, M. Isobe and T. Goto, *Bioorganic Chemistry*, 1989, **17**, 454-460.
22. F. Xu, X. N. Song, G. P. Sheng, H. W. Luo, W. W. Li, R. S. Yao and H. Q. Yu, *Separation and Purification Technology*, 2015, **142**, 18-24.
23. D. Briggs, D. M. Brewis, R. H. Dahm and I. W. Fletcher, *Surface and Interface Analysis*, 2003, **35**, 156-167.
24. T. Leefmann, C. Heim, A. Kryvenda, S. Siljestrom, P. Sjovall and V. Thiel, *Organic Geochemistry*, 2013, **57**, 23-33.
25. T. Leefmann, C. Heim, S. Siljestrom, M. Blumenberg, P. Sjovall and V. Thiel, *Rapid Communications in Mass Spectrometry*, 2013, **27**, 565-581.
26. S. Reichlmaier, J. S. Hammond, M. J. Hearn and D. Briggs, *Surface and Interface Analysis*, 1994, **21**, 739-746.
27. J. Qu, Y. M. Wang, G. A. Luo and Z. P. Wu, *Journal of Chromatography A*, 2001, **928**, 155-162.
28. M. K. Passarelli and N. Winograd, *Biochimica Et Biophysica Acta-Molecular and Cell Biology of Lipids*, 2011, **1811**, 976-990.
29. Y. Ding, Y. Zhou, J. Yao, C. Szymanski, J. K. Fredrickson, L. Shi, B. Cao, Z. Zhu and X. Y. Yu, *Anal Chem*, 2016.

30. V. Vaida, *Journal of Chemical Physics*, 2011, **135**.
31. J. R. R. Verlet, A. E. Bragg, A. Kammrath, O. Cheshnovsky and D. M. Neumark, *Science*, 2005, **307**, 93-96.
32. A. Sosnik, R. N. S. Sodhi, P. M. Brodersen and M. V. Sefton, *Biomaterials*, 2006, **27**, 2340-2348.
33. G. Bruny, S. Eden, S. Feil, R. Fillol, K. El Farkh, M. M. Harb, C. Teyssier, S. Ouaskit, H. Abdoul-Carime, B. Farizon, M. Farizon and T. D. Mark, *Review of Scientific Instruments*, 2012, **83**.
34. K. Keune and J. J. Boon, *Surface and Interface Analysis*, 2004, **36**, 1620-1628.
35. A. K. Gianotto, B. D. M. Hodges, M. T. Benson, P. D. Harrington, A. D. Appelhans, J. E. Olson and G. S. Groenewold, *Journal of Physical Chemistry A*, 2003, **107**, 5948-5955.
36. X. Hua, X. Y. Yu, Z. Y. Wang, L. Yang, B. W. Liu, Z. H. Zhu, A. E. Tucker, W. B. Chrisler, E. A. Hill, T. Thevuthasan, Y. H. Lin, S. Q. Liu and M. J. Marshall, *Analyst*, 2014, **139**, 1609-1613.
37. J. C. Vickerman, *Analyst*, 2011, **136**, 2199-2217.
38. U. Ceglarek, J. Efer, A. Schreiber, E. Zwanziger and W. Engewald, *Fresenius Journal of Analytical Chemistry*, 1999, **365**, 674-681.
39. M. Barco, C. Planas, O. Palacios, F. Ventura, J. Rivera and J. Caixach, *Analytical Chemistry*, 2003, **75**, 5129-5136.
40. M. Dizdaroglu, Z. Nackerdien, B. C. Chao, E. Gajewski and G. Rao, *Arch Biochem Biophys*, 1991, **285**, 388-390.
41. M. Karrasch, G. Borner, M. Enssle and R. K. Thauer, *Eur J Biochem*, 1990, **194**, 367-372.